RESEARCH ARTICLE

WILEY

A randomized controlled preclinical trial on 3 interposal temporomandibular joint disc implants: TEMPOJIMS—Phase 2

David Faustino Ângelo[1,2,3] 🄳 | Yadong Wang[4] | Pedro Morouço[5] |
Florencio Monje[6] | Lisete Mónico[7] | Raúl González-Garcia[6] | Carla Moura[3] |
Nuno Alves[3] | David Sanz[1] | Jin Gao[8] | Rita Sousa[2] | Lia Neto[2] |
Pedro Faísca[9] | Francisco Salvado[2] | Monica López Peña[10] | Maria Permuy[10] |
Fernando Munñoz[10]

[1]Instituto Português da Face, Lisboa, Portugal

[2]Faculdade de Medicina da Universidade de Lisboa, Lisboa, Portugal

[3]Centre for Rapid and Sustainable Product Development, Polytechnic Institute of Leiria, Leiria, Portugal

[4]Cornell University, Ithaca, New York, USA

[5]Polytechnic Institute of Leiria, Leiria, Portugal

[6]Complejo Hospitalario Universitario de Badajoz, Badajoz, Spain

[7]University of Coimbra, Coimbra, Portugal

[8]Department of Bioengineering, University of Pittsburgh, Pittsburgh, Pennsylvania, USA

[9]Gulbenkian Institute of Science, Oeiras, Portugal

[10]University of Santiago de Compostela—Lugo Campus, Lugo, Spain

Correspondence
David Faustino Ângelo, Instituto Português da Face Rua Tomás Ribeiro, no71 5oAndar, 1150-227, Lisboa, Portugal.
Email: david.serrano.angelo@gmail.com

Abstract

The effort to develop an effective and safe temporomandibular joint (TMJ) disc substitute has been one of the mainstreams of tissue engineering. Biodegradable customized scaffolds could approach safety and effectiveness to regenerate a new autologous disc, rather than using non-biodegradable materials. However, it is still technically challenging to mimic the biomechanical properties of the native disc with biodegradable polymers. In this study, new 3D tailored TMJ disc implants were developed: (1) Poly(glycerol sebacate) (PGS) scaffold reinforced with electrospun Poly(εcaprolactone) (PCL) fibers on the outer surface (PGS+PCL); (2) PCL and polyethylene glycol diacrylate (PEGDA) (PCL+PEGDA); and (3) PCL. The TMJ implants were tested in a randomized preclinical trial, conducted in 24 black Merino sheep TMJ, perfoming bilateral interventions. Histologic, imaging, and kinematics analysis was performed. No statistical changes were observed between the PGS+PCL disc and the control group. The PCL+PEGDA and PCL groups were associated with statistical changes in histology ($p = 0.004$ for articular cartilage mid-layer; $p = 0.019$ for structure changes and $p = 0.017$ for cell shape changes), imaging ($p = 0.027$ for global appreciation) and dangerous material fragmentation was observed. No biomaterial particles were observed in the multi-organ analysis in the different groups. The sheep confirmed to be a relevant animal model for TMJ disc surgery and regenerative approaches. The PCL and PCL+PEGDA discs presented a higher risk to increase degenerative changes, due to material fragmentation. None of the tested discs regenerate a new autologous disc, however, PGS+PCL was safe, demonstrated rapid resorption, and was capable to prevent condyle degenerative changes.

KEYWORDS
biomaterials, preclinical research, sheep, temporomandibular joint disc, temporomandibular joint disorders, tissue engineering

1 | INTRODUCTION

The modern temporomandibular joint (TMJ) surgical techniques are progressing to more advanced and minimally invasive treatments, such as TMJ arthroscopic disc repositioning with coblation and suture (Liu et al., 2018). However, classical techniques involving open surgery, such as TMJ discopexy (Abramowicz & Dolwick, 2010; Dolwick, 2001; Hall, 1984; McCarty & Farrar, 1979; Mercuri et al., 1982; Walker & Kalamchi, 1987) and TMJ discectomy (Bjørnland & Larheim, 2003; Candirli et al., 2017; Miloro et al., 2017) still play an important role on severe joint dysfunction cases. Temporomandibular joint open discopexy is mainly used in disc displacements, which have failed to respond to conservative, and minimally invasive treatments (Soni, 2019). Temporomandibular joint discectomy is mostly reserved for dysfunctional, deformed or perforated disc, which cannot be saved (Renapurkar, 2018). In Temporomandibular Joint Interposal Material Study (TEMPOJIMS) 1 (Ângelo et al., 2017), the authors have previously studied the functional (Ângelo, Gil, et al., 2018) and morphologic (Ângelo, Morouço, et al., 2018) TMJ changes after bilateral discectomy and discopexy in a randomized preclinical trial conducted in purebred black Merino sheep. According to TEMPOJIMS 1 (Ângelo et al., 2017; Ângelo, Morouço, et al., 2018; Renapurkar, 2018) and other clinical results, TMJ discectomy can induce significant degenerative changes (Bjørnland & Larheim, 2003; Candirli et al., 2017; Eriksson & Westesson, 1987; Hagandora & Almarza, 2012; Holmlund, 1993; Widmark et al., 1996, 1997), with osteoarthrosis (OA) and/or osteophytosis (Eriksson & Westesson, 2001; Holmlund, 1993). These undesirable results have highlighted the need for a TMJ disc substitute to protect the condyle and the temporal fossa from degenerative changes after discectomy. However, currently there are no effective and safe solutions to replace a damaged TMJ disc in humans, besides several attempts in the past had resulted in worsening rather than improving patient outcome (Schliephake et al., 1999; Spagnoli & Kent, 1992; Tucker & Burkes, 1989).

Many materials have been tested for TMJ disc replacement: (1) polyamide (Springer et al., 2001); (2) polyglycolic acid (PGA) (Wang et al., 2009); (3) flat discs of poly(glycerol sebacate) (PGS) (Chin et al., 2018); (4) polylactic acid (PLA) (Ahtiainen et al., 2013); (5) polytetrafluoroethylene (Lai et al., 2001); (6) silicone sheets (Hartman et al., 1988; Schliephake et al., 1999); (7) other biomaterials, such as collagen hydrogels and decellularized tissues (Brown et al., 2012; Li et al., 2017). However, none of these has progressed to clinical trials. Polytetrafluoroethylene has showed particle debris and breakdown (Alonso et al., 2009; Lai et al., 2001), and silicone sheets have showed decrease in condylar width, histiocytes accumulation and presence of T-lymphocytes results from foreign body response which lead to important safety concerns (Schliephake et al., 1999).

Poly(εcaprolactone) has been widely investigated in tissue engineering (TE), due to its slow degradation rate, for producing scaffolds, electrospun fibers or composites for cartilage TE, considering the slow rate of cartilage regeneration (Annabi et al., 2011; Dong et al., 2017; Garrigues et al., 2014). In addition to having excellent biocompatibility and adequate mechanical properties, it has not been tested as TMJ disc substitute in an adequate preclinical trial. Poly (ethylene glycol) diacrylate (PEGDA) hydrogels are also widely studied for cell encapsulation in order to repair cartilage damages in patients with OA (Musumeci et al., 2011, 2013). It is also known that PEGDA hydrogels suffer a slow in vitro hydrolytic degradation, reducing degradation rate, enabling them for a long-term implant (Choi et al., 2019). This degradation happens due to the cleavage of its ester linkage. Browning group reported a significant in vivo degradation of PEGDA hydrogels within 12 weeks (Browning et al., 2014). In our biomechanical analysis, the PEGDA disc failed in the loading tests. We reinforced the PEGDA discs with PCL to mimic native disc biomechanics. This material was not tested previously in a preclinical trial. In 2013, Hagandora and collaborators referred that PGS was a novel scaffold material for TMJ disc engineering. Poly (glycerol sebacate) is described as a biocompatible, biodegradable elastomer with great potential as a scaffold material for TMJ disc engineering (Hagandora et al., 2013). The PGS disc was reinforced with PCL to mimic native disc biomechanics.

In this study, the authors tested the efficacy of three different biodegradable interposal TMJ disc implants featuring a 3D geometry and biomechanics properties of the native TMJ disc: (1) PGS scaffold reinforced with electrospun PCL fibers on the outer surface (PGS +PCL); (2) PCL and PEGDA (PCL+PEGDA) and (3) PCL. The study protocol of this rigorous preclinical trial was previously published (Ângelo et al., 2017) as recommended in the ARRIVE guidelines, and was designed to improve the quality of preclinical trials in this domain, contributing to improve the safety of future TMJ interposal biomaterials. We believe this is the first report on PCL, PEGDA and PGS in combination with PCL tested in a randomized preclinical trial in sheep, as a large animal model to promote translational studies to humans.

2 | MATERIALS AND METHODS

2.1 | Interposal biomaterials engineering

2.1.1 | Disc design and production

The TMJ disc anatomy of adult black Merino sheep was studied in 2016. The mean length and width of the discs were 21.23 mm (SD = 1.53) and 11.49 mm (SD = 0.62), respectively. Anterior and posterior band thicknesses were 1.05 mm (SD = 0.07) and 1.27 mm (SD = 0.04), respectively. Mean central thickness was 0.76 mm (SD = 0.09) (Angelo et al., 2016). TMJ disc scanning was perfomed to obtain a 3D virtual model with rigorous geometry.

PCL disc
The PCL disc (Figure S1A), with a molecular weight of 50 kDa, was used (MW 6500, Perstorp) (Morouço et al., 2016). The 3D scaffolds were produced using a BioExtruder®, by fiber deposition with

300 μm of diameter, 350 μm of pore size, and 0°/90° lay-down pattern. The system was heated to 78°C to fuse the material. For its extrusion, the deposition spindle was 10.5 rpm and the crosshead speed was 9 mm s^{-1}.

PCL+PEGDA disc

Poly(ethylene glycol) diacrylate (MW 575, Sigma-Aldrich®) hydrogels were produced in a concentration of 20% w/V, dissolved in the aqueous solution of 0.5 M of 2-[4-(2-hydroxyethyl) piperazin-1-yl] ethanesulfonic acid buffer (Sigma-Aldrich®). Photopolymerization was induced through the addition of 0.1% w/V 2.2-dimethoxy-1.2-diphenylethanone (DMPA, Sigma-Aldrich) photoinitiator to 10 ml of PEGDA solution in a transparent petri dish, followed by UV light (λ = 365 nm) exposure. Hydrogel formation took about 3 min to full exhaustion of the acetylate groups. The PCL scaffolds were produced as previously mentioned, and then, a layer of PEGDA was photo-polymerized surrounding the PCL scaffold, forming a sandwich-type of composite structure (Figure S1B).

PGS+PCL disc

Prior report of PGS implants were of flat sponges (Chin et al., 2018). Here we made the implant matching the shape of the native sheep TMJ disc. Poly(εcaprolactone) was added to PGS disc (Figure S1C) in a porous scaffold prepared by a modified salt fusion method. Ground salt particles (150 mg) with a size range of 25–32 μm were placed into the sheep disc 3D printed mold. The mold was transferred to an incubator at 37°C and 90% relative humidity for 1 h. The fused templates of salt particles were dried in a vacuum oven at 90°C and 100 millitorr (mTorr) overnight, removing salt cake carefully from the mold before further processing. Fresh-made PGS+PCL dissolved in tetrahydrofuran (THF; 20 wt%, 380 μL, salt: PGS+PCL = 2:1) was added to the salt cake, and the THF was allowed to evaporate completely in a fume hood for 30 min. The salt cake was transferred to a vacuum oven and cured at 150°C and 100 mTorr for 24 h. The resultant PGS+PCL impregnated salt templates were soaked in deionized water for 4 h and then replaced with water for 4 h, with water exchange every 4 h during the first 12 h. After the 12 h water bath, scaffolds were transferred to deionized water for another 24 h with water exchange every 8 h. The resultant scaffolds were frozen down at −80°C and then the lyophilization process was applied. The scaffolds were performed by 70% soaking, then followed by 50%, 25% ethanol plus Milli-Q water rinsing to remove the impurities before electro-spinning. To fabricate the PCL layer, PCL polymer was dissolved (Sigma) in 2.2.2-trifluoroethanol (TFE, ACROS) at 14% W/V and electrospun the solution onto the rotating PGS+PCL disc. Electrospinning solution was delivered via a syringe pump (NE-1000, New Era Pump Systems Inc.) for controlling the mass flow rate (25 μL min^{-1}), the electrical strength applied for electrospinning PCL was 12 kV cm^{-1}. The Eletrospinning method is depicted in (Figure S2) The resultant scaffolds with 50 μm PCL fiber were then transferred to vacuum oven at 50°C for 4 h to remove TFE and enhance fiber fusion, PGS+PCL scaffolds were sterilized γ–radiation.

2.1.2 | Scanning electron microscopy analysis

Scanning Electron Microscopy was performed to all the discs before surgery (Figure 1).

2.2 | In vivo study design

The rationale and protocol of TEMPOJIMS is published in the study of Ângelo et al. (2017). The present study was approved by the Portuguese National Authority for Animal Health and registered with the number 026618. The care and handling of sheep conformed to the requirements of the animal care and use ethical committee of University of Lisbon.

2.2.1 | Study population and sample

The animal model selected to conduct this investigation was the sheep. To reduce biological variability, the authors performed this study in a black Merino sheep strain (Angelo et al., 2016). The authors used black Merino sheep with the following inclusion criteria: certified black Merino sheep pure bred, adult (aged between 2 and 5 years), female, good health condition (veterinary checks were performed on all animals), and normal dentition.

2.2.2 | Randomization

The randomization process was achieved by a statistical group not tackled in the outcome assessments. In phase 2, 10 sheep were randomly allocated to each intervention group: bilateral PCL interposal biomaterial group (n = 3), bilateral PCL+PEGDA interposal biomaterial group (n = 3), bilateral PGS+PCL interposal biomaterial group (n = 3) and backup group (n = 1). One backup sheep was planned to be used if death occurred due to anesthesia or other difficulties not related to surgical intervention. The discopexy group (n = 3) is a historical control used in TEMPOJIMS phase 1 (Ângelo, Gil, et al., 2018). The allocation to each randomized group was performed preoperatively by sealed envelope.

2.3 | Intervention phase

Ten eligible sheep were assigned to their baseline secondary outcomes measured at days 11, 10, and 9 before surgery in central TEMPOJIMS facilities. Transportation to surgical facilities was performed 5 days before surgery to avoid animal stress and allow familiarization to temporary accommodations. The surgical team was not blinded to treatment allocation given the type of intervention. However, surgical team members were not involved in outcome assessment. Serious adverse events were defined as occurrences that were fatal, or life-threatening or persistent disability, which resulted
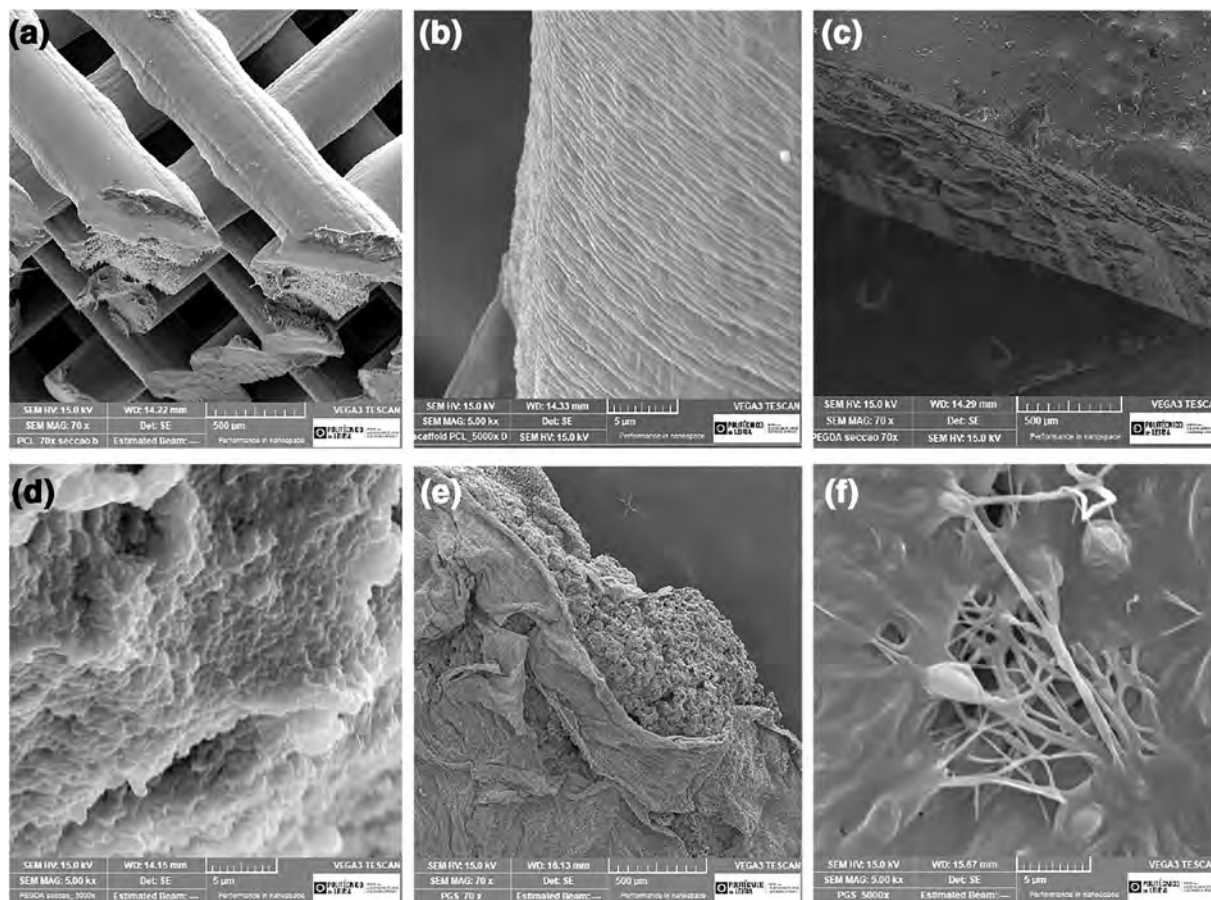
FIGURE 1 Scanning electron microscopy analysis 15.0 kV. (a) Poly(εcaprolactone) (PCL) disc 70x amplification. (b) PCL disc section 5000x amplification. (c) Poly(ethylene glycol) diacrylate (PEGDA) disc section 70x amplification (d) PEGDA disc 5000x amplification. (e) Poly(glycerol sebacate) (PGS) disc 70x amplification (f) PGS disc 5000x amplification

in death, more than 10% weight loss per week, or clinically significant hazard or harm to the animal.

2.3.1 | Anesthesia protocol

Fasting and water restriction were required 24 h before surgery. Sedation was performed with diazepam (0.5 mg kg^{-1} i.v.), followed by anesthesia induction with ketamine (5 mg kg^{-1} i.v.). Oral intubation was performed, and anesthesia was maintained with isoflurane (1.5% to 2%). To assure animal analgesia, meloxicam (0.5 mg kg^{-1} i.v., bid) was administered in surgery day and for 4 days post-operatively. Antibiotic prophylaxis with amoxicillin and clavulanic acid were administrated for 5 days.

2.3.2 | Surgical intervention

Trichotomy of the surgical site was performed and the skin was prepared with a povidone-iodine solution. Sterile surgical drapes were placed to isolate the surgical site. Two per cent lidocaine local anesthetic with vasoconstrictor (1:100,000) was infiltrated in the subcutaneous tissues. A preauricular incision was performed with a 15 blade scalpel, the skin and subcutaneous tissues were dissected with a Metzenbaum scissor until reaching the TMJ lateral ligament and capsule. An incision was performed to access the upper compartment and the disc was identified. The medial, anterior, posterior, and lateral disc attachments were desiccated with the monopolar electrosurgery equipment and discectomy was performed. The PCL, PCL+PEGDA or the PGS+PCL scaffolds (n = 6 for each group) were bilaterally interposed between the condyle and temporal fossa respectively to substitute the previous native disc (Figure 2a–d). A PDS 3-0 suture was used to attach the disc anteriorly and posteriorly. The capsule was closed with vicryl 4-0. The wound was closed in layers with vicryl 3-0.

2.4 | Follow-up assessments

Baseline assessment (T0) was performed before surgery on days 11, 10, and 9. Ten days after surgery, animals were transported to TEM-POJIMS facilities. Follow-up recording of kinematics and body mass outcomes began on days 19, 20 and 21 after surgery (T1) and it was repeated on the same days for the next 5 months. T0–T6 were based on

FIGURE 2 Surgical intervention.
(a) Exposing temporomandibular joint (TMJ)
upper compartment. (b) Exposing TMJ lower
compartment. (c) After discectomy, interposing
de TMJ interposal biomaterial. (d) TMJ
interposal biomaterial interposed between the
condyle and temporal fossa
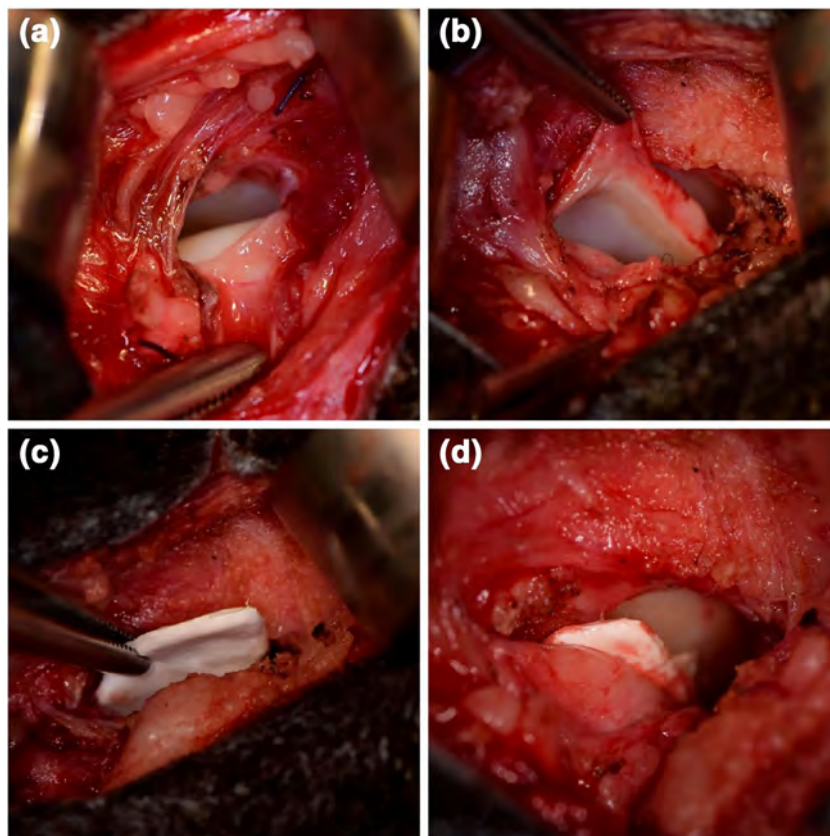
the means of the three measurements. For kinematics, 4 principal outcomes were collected: (1) absolute masticatory time; (2) rumination time per cycle; (3) rumination kinematics and (4) rumination area and geometry. Temporomandibular joint and organs were explanted on day 185, and stored for histological and imaging analysis (Figure S3).

2.4.1 | Kinematic analysis

To measure the attributed outcomes a series of stages were performed. Once the sheep was inside the cage, a dose of 150 g of dry pellets (Rico Gado A3) was placed in the feeder and time was measured with a chronometer (absolute masticatory time). The rumination time per cycle was obtained by recording 15 rumination cycles and tracking the jaw movement obtaining the ruminant cycle. One cycle was obtained by using a 25 frames per second video camera (Canon 7D) divided by 25. The rumination area and geometry were assessed through a 2D tracking software which calculates the average ruminant cycle, and then the after-effects software converts the 2D into a geometric form.

2.4.2 | Body mass analysis

Sheep were weighted after eating 150 g of dry pellets. Body mass assessments were performed by two trained evaluators who were not affiliated with the interventions.

2.5 | Histologic analysis

Intact TMJ was removed using a necropsy bone oscillatory saw according to the following anatomic references: (1) cranial: cranial aspect of the coronoid process in the union region of the zygomatic process; (2) caudal: external to acoustic meatus; (3) dorsal: the squamous temporal bone and (4) ventral: 2 cm below the acoustic meatus in the zone of stylo-hyoid angle. After storage in 10% formalin, the joints were coded and shipped to The Veterinary Faculty of the University of Santiago de Compostela (Lugo, Spain), and the histological processing and evaluation was performed. The TMJ joints were processed for ground sectioning in conformity with the method described by Donath and Breuner (Poveda et al., 2007). The samples were dehydrated in ascending grades of ethanol, infiltrated and embedded with a light curing resin (Technovit 7200-VCL, Heraus Kulzer GmbH, Werheim, Germany). From each TMJ one section was prepared and reduced to a thickness of approximately 40 μm using a grinding machine (Exact Apparatebau). The slides obtained were stained using Levai Laczkó technique (Poveda et al., 2007). Samples were histological analyzed by two blinded independent examiners with experience in OA evaluation. These examiners also scored discopexy samples from TEMPOJIMS phase 1 (Ângelo, Gil, et al., 2018).

The analysis was performed initially, making a histologic description of the principal features observed in the samples, with emphasis in cartilage structure, chondrocyte number and shape and

presence of clusters in both temporal and mandibular surfaces. Also was observed those parameters separately in superficial and deep layer of the non-calcified and calcified cartilage. In subchondral bone the main structure was identified, and parameters related to the bone remodeling as vascular invasion, osteoblast activation, as well as, the presence of mature osteocytes. Later, those observations were transferred to a rank order were 0 was normal and 3 the most altered (Table S6).

2.6 | Imaging analysis

Temporomandibular joint blocks were scanned by computed tomography (CT) and imaging evaluation was performed and classified independently by two experienced radiologists (Rita Sousa, Lia Neto) who were blinded to the intervention using the criteria and score previously described by the author (Ângelo et al., 2017).

2.7 | Euthanasia and multi-organ histologic analysis

2.7.1 | Euthanasia protocol

In accordance with directive 2010/63/eu of the European parliament and the council of September 22, 2010 and Portuguese decree-law n° 113/2013 of August 7 the authors performed the euthanized in the accommodation site, one animal at each time by barbiturate overdose. Intramuscular administration of 1.5 mg kg^{-1} Midazolam was injected in the neck muscles for sedation. In some animals, for deep sedation the authors performed additionally 1 mg kg^{-1} Diazepam intramuscular injection. Once sedated, rapid intravenous injection of 0.4 ml kg^{-1} Sodium Pentobarbital (Euthasol vet. 400 mg ml^{-1}) through jugular vein was performed. The authors confirmed death after euthanasia by observing no respiratory movement for at least 3 min, and no heartbeat (using a stethoscope), lack of pulse and corneal reflex, graying of the mucous membranes, and rigor mortis.

2.7.2 | Multi-organ analysis

Data from cadavers with hip or knee alloplastic replacement show generally high concentrations of particles in the liver, spleen, kidneys and lymph nodes (Urban et al., 2000). Silicone disc substitute have also been associate with migration of this material into adjacent tissues. To evaluate safety of the interposal biomaterials tested, after euthanasia the authors dissected and histopathologic analyzed the following organs: brain, cervical lymphonodes, parotid gland, submaxillary gland, hearth, lungs, liver, kidneys and spleen (Figure S4).

2.8 | Statistical analysis

2.8.1 | Primary outcome

Histological statistical analysis
Results were expressed as medians. The statistical comparison of the four groups was performed using the Kruskal–Wallis One-way Analysis of Variance (ANOVA) on Ranks. The level os statistical significance used was $p < 0.05$. The post-hoc test analysis was done using Dunn's test. All statistical analyses were performed using commercially available software Sigma Plot 12.5 (Systat Software Inc.).

2.8.2 | Secondary outcomes

Imaging statistical analysis
The authors evaluated the following outcomes: Shape, Condyle erosion, Temporal erosion, Condyle sclerosis, Temporal sclerosis, Condyle marrow, and Temporal marrow. Non-parametric tests were performed attending to the sample size and the non-normality of the distribution for most variables in each group, Shapiro–Wilk tests ≤0.87, $0 < p < 0.212$. Kruskal–Wallis tests were performed for group comparisons, with Bonferroni test for post-hoc test multiple comparisons. Partial eta squared (η_p^2) and Cohen's D were used for effect size calculations. Cohen's categories were used to evaluate the magnitude of these effect sizes (small if $0 < |d| < 0.5$, medium if $0.5 < |d| < 0.8$, and large if $|d| > 0.8$). Data analyses were performed using SPSS, version 22.0.

Body mass statistical analysis
To analyze body mass (weight) results, normality tests were performed with Shapiro–Wilk in each time (T0–T6) and in each group, showing that the outcome variables in pre-hoc (T0) and post-hoc test (T1–T6) have a normal distribution, $p \geq 0.094$. An exception was found for PGS+PCL in the pre-hoc test and in time three of the post-hoc test ($p < 0.001$), and Kruskal–Wallis and Friedman tests were performed for PGS+PCL to check same sample in different time periods. Error variances of the dependent variables were tested with Levene's Test of Equality of Error Variances, showing variances equal across groups, $p \geq 0.055$.

For cross-sectional analysis a one-way ANOVA was performed, to compare body mass in the four randomized groups before and after the random treatment group assignment. For longitudinal analysis, a one-way ANOVA with repeated measures was performed taking as within-subjects effects observations postoperative (T1–T6) for all conditions. The tests of within-subjects contrasts were performed in comparison with the baseline (T0). Estimates of effect size were calculated using partial eta squared (η_p^2). Observed power was calculated with $1 - \beta$'s score. Body mass was measured three times in the pre-hoc test for supporting invariance concerning the outcome

measures before the clinical intervention. The post-hoc test analysis assessed body mass measuring three times, in six time-points (T1–T6), one per month at the same place, date and hour as in TEMPO-JIMS phase 1.

Kinematic statistical analysis

The primary analysis tested the effects of the independent variable for three different interposal biomaterials: (A) PCL bilateral interposal biomaterial; (B) PCL+PEGDA bilateral interposal biomaterial and; (C) PGS+PCL bilateral interposal biomaterial; (D) bilateral discopexy (TEMPOJIMS phase 1), using a series of pre-hoc tests (T0) and post-hoc tests (T1–T6). Randomized pre-hoc and post-hoc tests were used to evaluate the effects of surgical intervention. Three measures were performed in the pre-hoc test, supporting invariance concerning the outcome measures. All statistical analyses were performed with SPSS, version 22.0. For all analyses a probability of type I error (α) = 0.05 (95% confidence interval) was considered. Normality tests were performed with Shapiro–Wilk for each group in pre-hoc and post-hoc tests (T1–T6), showing that the outcome variables have a normal distribution, S-W (3) $\geq$ 0.774, $p \geq 0.054$. Analysis of variance was performed for group comparisons. Error variances of the dependent variables were tested with Levene's Test of Equality of Error Variances, showing equal variances across groups ($p \geq 0.098$) except for T1 in absolute masticatory time (Levene statistics = 5.26, $p = 0.03$), which led to non-parametric tests being calculated for this time.

Measures in the pre-hoc test showed that the sheep did not change across time until the data of the surgery, $p > 0.50$. Bonferroni test was used for post-hoc test for multiple comparisons and Dunnett test for comparisons with the control group (bilateral discopexy). Partial eta squared (η_p^2) and Cohen's D were used for effect size calculations. Cohen (1988) defined effect sizes as "small, $d = 0.2$," "medium, $d = 0.5$," and "large, $d = 0.8$" ($p = 0.25$). To avoid bias in data analysis, for animals with no rumination after surgery was assumed: (1) zero for rumination area and (2) the double of the highest score for rumination time per cycle. Cohen's D is used to reduce the dimension bias associated with different sheep mandible physiology.

3 | RESULTS

3.1 | Histological study

3.1.1 | Poly(εcaprolactone)

In the PCL group only five samples were evaluated due to the loss of a sample during the processing. In those five samples, the interposal biomaterial was present after 6 months. Extensive condyle osteolysis in four-fifths samples (Figure 3a). Most of the non-hyaline cartilage of both surfaces was substituted by fibrous-like tissue (more than 70% of the non-hyaline cartilage was missing) in four-fifths samples. Two samples presented a foreign body reaction with presence of giant
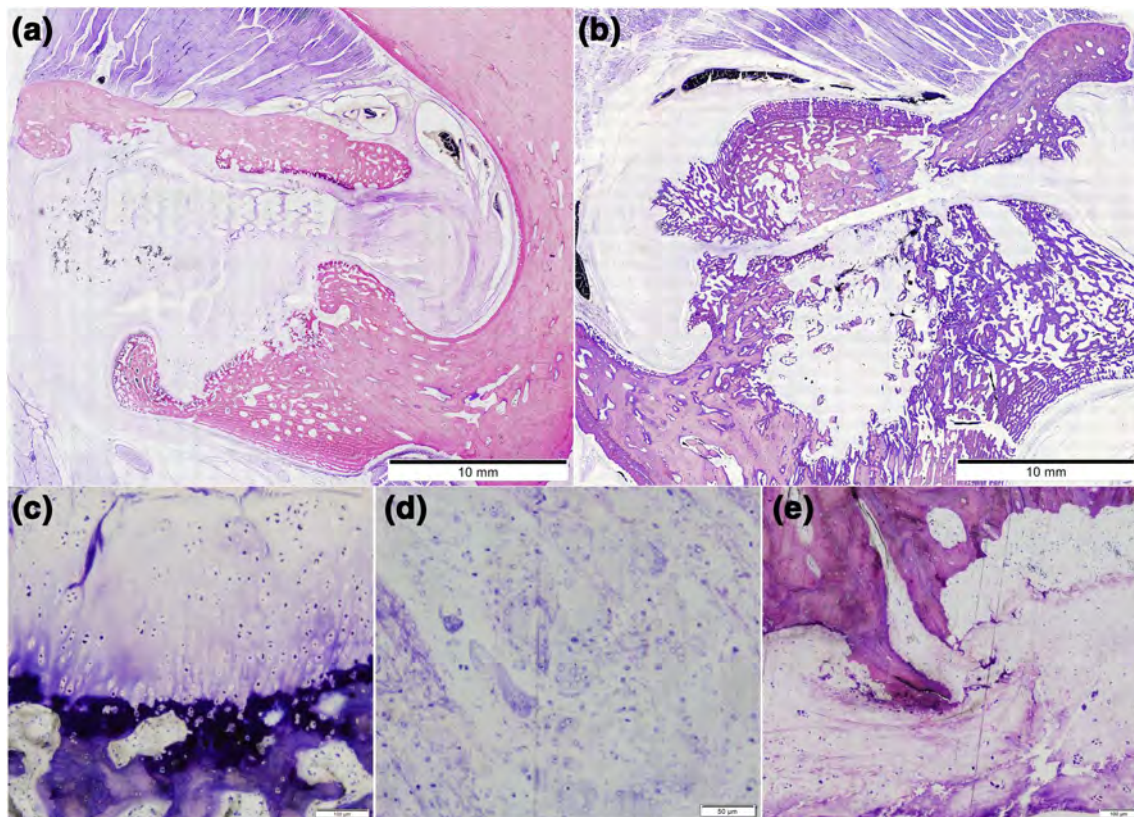

FIGURE 3 (a) Extensive osteolysis with poly(εcaprolactone) (PCL) disc. (b) Osteolysis and disc fusion with poly(glycerol sebacate) + PCL. (c) Cluster formation and cell reduction. (d) Foreign body reaction with the presence of giant cells. (e) Cluster formation and cell reduction

cells (Figure 3d). Due to the absence of the non-hyaline cartilage most of the features could not be evaluated. Only in one sample, almost 50% of the calcified and non-calcified cartilage of the temporal surface was still present. In this case in the non-calcified cartilage draws attention then the deep layer has fibers oriented parallel to bone surface rather than the normal perpendicular disposition. When non-hyaline cartilage is present, we observed cell diminution and some clustering formation (Figure 3e). Subchondral bone presented osteolytic areas in four-fifths samples.

3.1.2 | Poly(εcaprolactone) + Poly(ethylene glycol) diacrylate

The biomaterial was still present in five of the six samples. The non-calcified cartilage was absent in more than the 70% of their extent in both articular surfaces (mandibular and temporal) in five-sixths samples being substituted by a fibrous-like tissue in three of them. In all the samples analyzed, the number of cells in the superficial layer of the non-calcified cartilage were reduced but the cells present presented a normal shape and do not form clusters except in one case. In the deep layer, the structure was also altered with fewer cells, not organized in columns, as in normal cartilage, and with cluster formation in both surfaces of the same sample (Figure 3e). The calcified layer was altered in both surfaces of five samples being in most of the cases almost absent. Finally, the subchondral bone presented a high rate of remodeling in half of the samples (3/6 in mandibular bone and 4/6 in temporal bone). When altered, mandibular bone presented high remodeling with structure alteration, but in one sample the temporal bone structure was considered normal with only mild alteration in osteoblast activation and vascular invasion. The other three revealed altered samples of temporal bone with abnormal bone remodeling.

3.1.3 | Poly(glycerol sebacate) + Poly(εcaprolactone)

In all cases, we observed a total reabsorption of the interposal biomaterial. There was one sample with high osteolysis with no calcified cartilage and with the non-calcified cartilage partially fused between both surfaces (Figure 3b). In the other five samples, the non-calcified cartilage was present in all the samples in different degrees. In two was present in more than 70% in both surfaces, in three in almost 50%. In all the samples there was cluster formation and cell diminution (Figure 3c). The calcified cartilage was present in the same degree as the non-calcified one. In two samples was described as normal and in other two it was thin but with normal or diminished number of cells. In the other one, the number of cells was increased respect to the normal cartilage. With respect to the subchondral bone, it was normal or with a mild remodeling in all the samples except the one with the osteolysis. The mild remodeling processes seen in the samples could correspond to suitable bone remodeling.

A comparing overview of histologic samples can be observed in Figure 4.

3.1.4 | Histological statistical results

With respect to the statistical comparison of histologic features, the authors compared discopexy, PCL, PCL+PEGDA and PGS+PCL groups in mandibular and temporal surfaces of the TMJs. The statistically significant results ($p < 0.05$) are exposed in Figures S5–S7).

In the condylar surface of the mandible, the authors found in cartilage superficial layer (AC lamina) the presence of cloning was statistically different ($p = 0.026$) among groups with difference by Dunn's method between PGS+PCL and PCL+PEGDA but not in the others. In the evaluation of the cell shape in the AC lamina the ANOVA on ranks gave statistical significance ($p = 0.036$) but was impossible to isolate the groups with differences with the Dunn's method.

Also, in the mandibular surface but in the deep non-calcified cartilage (AC mid-layer) the structure was statistically significant ($p = 0.004$). In this case when the authors isolate the groups that differ from the others using multiple comparisons, no differences were found between any of them.

In the mandibular calcified layer the comparison of the median values of the groups found statistical differences in structure ($p = 0.019$) and cell shape ($p = 0.017$) but in the pairwise multiple comparison only was found statistical difference only between PCL and discopexy in structure. Finally, with respect to subchondral bone parameters differences in structure ($p = 0.033$), osteoblast activation ($p = 0.015$) and vascular invasion ($p = 0.015$) were found with the Kruskal–Wallis ANOVA on ranks but only between discopexy and PCL in both osteoblastic and vascular parameters.

On the temporal surface, differences were found in AC lamina cell number ($p = 0.016$), in osteoblast activation and vascular invasion in the subchondral bone $p = 0.024$ and $p = 0.018$ respectively. When Dunn's method was applied, only in both subchondral bone parameters differences were found between PCL and discopexy.

3.2 | Imaging study

3.2.1 | CT analysis

The authors compared the nine outcomes between discopexy, PCL, PCL+PEGDA, and PGS+PCL conditions (Table 1). For global appreciation, effect size of the differences were about, eta squared $\eta_p^2 = 41.4\%$, statistical power $(1 - \beta) > 0.999$. Differences between the four groups were not statistically significant for condyle marrow, temporal marrow, and calcification ($p > 0.10$). For each of the remaining outcomes, and considering a Type I error = 0.10, differences were higher for shape ($p = 0.002$), followed by temporal erosion ($p = 0.016$), condyle erosion ($p = 0.066$, condyle sclerosis,
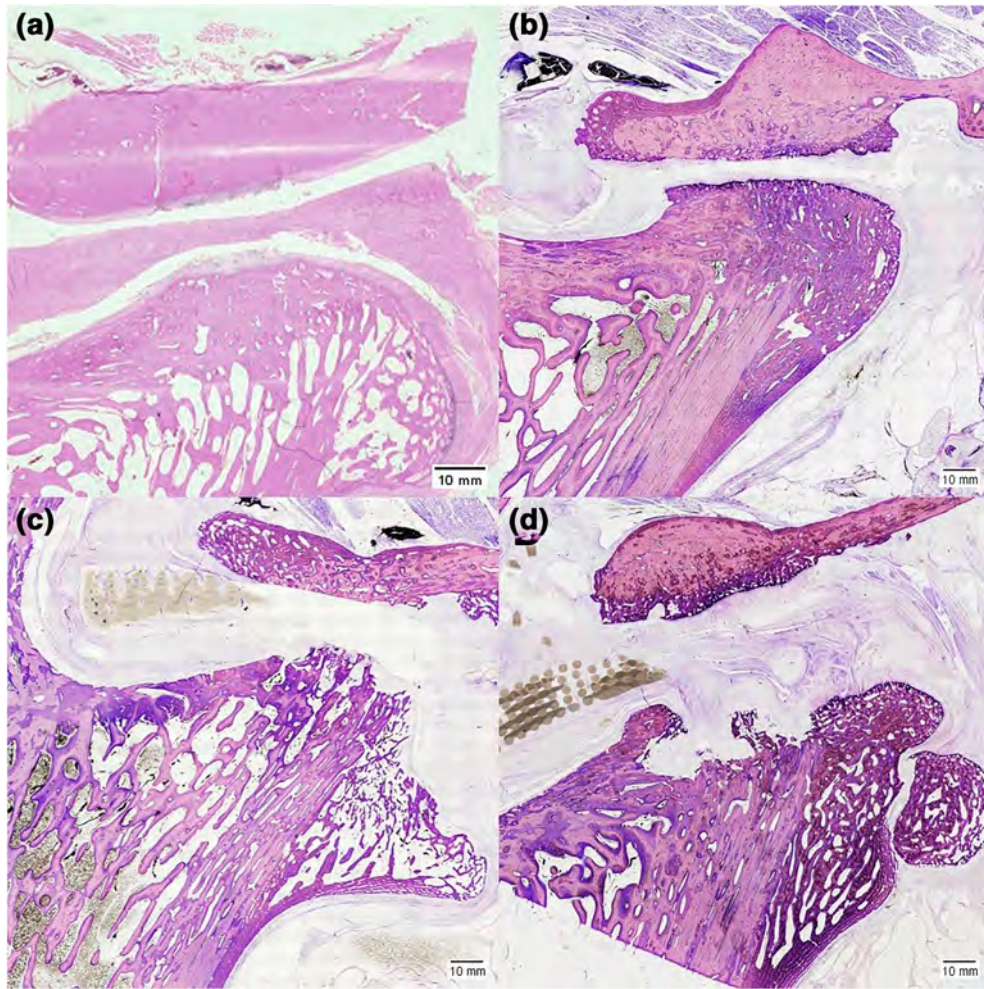
FIGURE 4 (a) Discopexy (control group—obtained from Temporomandibular Joint Interposal Material Study phase 1). (b) Poly(glycerol sebacate) + Poly(εcaprolactone) (PCL) disc. (c) PCL + poly(ethylene glycol) diacrylate disc. (d) PCL disc

and, at last, temporal sclerosis. The effect size of these differences ranges from 29.4% to 63.8%. In general, the scores of PCL, PCL+PEGDA, and PGS+PCL were higher compared to the discopexy. These effects are depicted in Figure 5.

In Table S1 it is presented the mean differences between discopexy, PGS+PCL, PCL+PEGDA, and PCL conditions. Discopexy only significantly differed from PCL+PEGDA for global appreciation (effect size of $R^2 = 40.5\%$), mainly due to shape (effect size of $R^2 = 80.4\%$), but also to temporal erosion ($R^2 = 50.2\%$) and condyle erosion ($R^2 = 16.5\%$). Discopexy did not significantly differ from PGS+PCL and PCL. According to Cohen's D score, a large effect size is considered if $d > 0.80$. Following this classification, the authors also found lower scores for discopexy in comparison with PCL for shape ($R^2 = 26.4\%$), Temporal erosion ($R^2 = 22.3\%$), Condyle sclerosis ($R^2 = 22.3\%$), and Condyle erosion ($R^2 = 19.0\%$). Apart from the temporal erosion ($R^2 = 22.3\%$), discopexy and PGS+PCL were the groups with no apparent differences (effect sizes between 0.0% and 10.0%).

The mean scores for each outcome and for the global appreciation are shown in Figure S8.

3.3 | Body mass results

Cross-sectional analysis. Global statistical differences (Bonferroni and Dunnett test) were not found in body mass in the pre-hoc test (T0) and in all times for the post-hoc test ($p \geq 0.876$) (Table S2). However, in Figure S9 can be seen that in the PGS+PCL condition sheep lost weight from T0 to T1, and then recovered their weight during T5 and T6.

A one-way ANOVA with repeated measures was performed taking as within-subjects effects months after surgery (T1–T6) for each group (PGS+PCL, PCL+PEGDA, PCL, and discopexy). Statistically significant differences were found mainly for discopexy [$F (5, 10) = 27.35$, $p < 0.001$, $\eta_p^2 = 0.932$, $(1 - \beta) > 0.999$], PGS+PCL [$F (5, 10) = 9.53$, $p = 0.001$, $\eta_p^2 = 0.826$, $(1 - \beta) = 0.991$], and with a lower effect size for PCL [$F (5, 10) = 3.18$, $p = 0.057$, $\eta_p^2 = 0.614$, $(1 - \beta) = 0.650$], showing that sheep recovered weight from T1 to T6. For PEGDA+PCL differences from T1 to T6 were not statistically significant, $F (5, 10) = 0.39$, $p = 0.847$, $\eta_p^2 = 0.162$, $(1 - \beta) = 0.110$.

The tests of within-subjects contrasts with the baseline (T0). Significant contrasts is identified in PCL+PEGDA for T2, T3, T4, and

TABLE 1 Means, standard deviations, means rank, Kruskal–Wallis tests, and effect sizes (η_p^2) for the outcomes

Group	Shape			Condyle erosion			Temporal erosion			Condyle sclerosis			Temporal sclerosis			Condyle marrow			Temporal marrow			Calcification			Global appreciation		
	M	SD	MR	M	SD	MR	M	SD	MR	M	SD	MR	M	SD	MR	M	SD	MR	M	SD	MR	M	SD	MR	M	SD	MR
PGS+PCL	1.17	0.41	7.92	1.17	0.98	11.67	0.67	0.52	12.33	1.00	0.63	7.83	0.67	0.52	9.33	1.17	0.98	10.50	0.83	0.98	11.00	0.00	0.00	11.50	1.17	0.41	8.83
PCL+PEGDA	2.83	0.41	20.00	2.00	0.89	17.17	1.50	0.84	18.50	1.83	0.75	15.33	1.33	0.52	16.50	1.50	0.84	12.92	1.67	0.82	17.08	0.17	0.41	13.50	2.17	0.75	18.00
PCL	2.00	0.89	14.17	1.50	0.55	14.00	0.67	0.52	12.33	1.83	0.41	16.17	1.00	0.00	13.00	1.83	0.41	15.33	1.00	0.89	12.17	0.17	0.41	13.50	1.67	0.52	14.33
Discopexy	1.17	0.41	7.92	0.67	0.52	7.17	0.17	0.41	6.83	1.33	0.52	10.67	0.83	0.41	11.17	1.33	0.82	11.25	0.67	0.82	9.75	0.00	0.00	11.50	1.17	0.41	8.83
$X^2(3)$	14.39**			7.19***			10.36*			6.92***			6.70***			2.22			4.28			2.09			9.20*		
p-value	0.002			0.066			0.016			0.075			0.082			0.528			0.233			0.554			0.027		

Abbreviations: M, means; MR, means rank; PCL, poly(ɛcaprolactone); PCL+PEGDA, poly(ɛcaprolactone) + poly(ethylene glycol) diacrylate; PGS+PCL, poly(glycerol sebacate) + poly(ɛcaprolactone); SD, standard deviations.

***$p \leq 0.082$; *$p \leq 0.05$; **$p \leq 0.01$.

T6, $p \leq 0.044$, and with a lower effect size in T1 ($p = 0.063$). For PCL, excluding T6 ($p = 0.109$) and considering a p-value < 0.10, significant contrasts were found in all times. In the discopexy group, significant differences were found in T5 ($p = 0.033$) and T6 ($p = 0.038$), and with a lower effect size in T1 ($p = 0.82$). For PGS +PCL the Friedman's non-parametric test showed a significant effect across time, $X^2(6) = 17.56$, $p = 0.007$, in which we verify a weight decrease in T1, and a significant increase from T1 to T6, $X^2(5) = 14.90$, $p = 0.011$.

3.4 | Kinematic results

Baseline descriptive statistics are in Table 2, with measurements of four chosen parameters, weight, absolute masticatory time, ruminant kinematics area, and ruminant time per cycle. The analyses might reveal pain in TMJ joint if the animal was increasing or decreasing on the different parameters.

Cross-sectional and longitudinal analyses were performed for both absolute masticatory time, rumination time per cycle, and rumination kinematics area. We used cross-sectional analysis to compare different interposal biomaterial groups of a single point in time, and it allowed the comparison of many different variables at the same time. However, it might not provide definite information about cause-effect relation. Firstly, a cross-sectional analysis establishes possible associations between the different variables, and on the longitudinal analysis the authors studied the cause and the effect. On the longitudinal analyses, the authors conducted several observations of the same interposal biomaterial groups over the follow-up period. The authors intend to observe individual developments in chosen characteristics for both interposal biomaterial groups.

3.4.1 | Absolute masticatory time

This parameter was based on the time taken by each animal to eat a dose of 150 g of dry pellets (Rico Gado A3).

Cross-sectional analysis: an ANOVA was performed, showing significant differences between the four groups only in T2, $F(3, 8) = 6.74$, $p = 0.014$, $\eta_p^2 = 0.717$, $(1 - \beta) = 0.847$. Dunnett post-hoc test in T2 showed a significant difference between PCL and discopexy group (Mean difference = 32.00, standard error [SE] = 9.95, $p = 0.030$), indicating an absolute masticatory time significantly higher in PCL interposal biomaterial group. Bonferroni test also showed significant higher scores for PCL in comparison with PGS+PCL (Mean difference = 40.44, SE = 9.95, $p = 0.022$) and with PCL+PEGDA(Mean difference = 35.11, SE = 9.95, $p = 0.046$).

Longitudinal analysis: a one-way ANOVA with repeated measures was performed, taking as within-subject effects preoperative (T0) and postoperative (T1 to T6) for PGS+PCL, PCL, PCL+PEGDA, and discopexy group (Figure S10). Significant effects across time were found mainly for PCL [$F(6, 12) = 11.64$, $p < 0.001$, $\eta_p^2 = 0.853$, $(1 - \beta) > 0.999$],
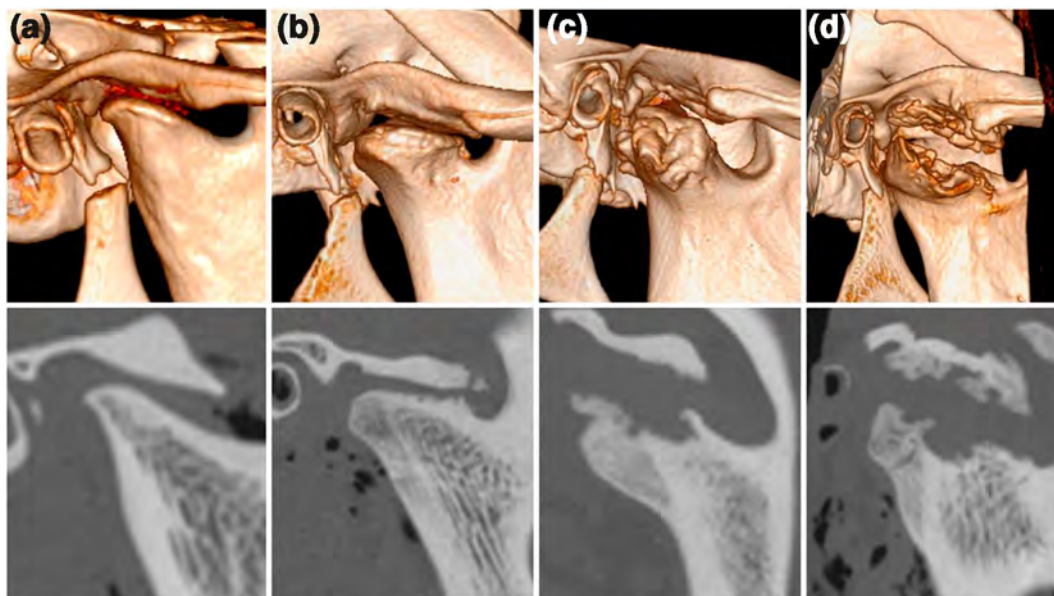
FIGURE 5 Representative computed tomography sagittal image of temporomandibular joint. (a) Control group—obtained from Temporomandibular Joint Interposal Material Study phase 1. (b) Poly(glycerol sebacate) + poly(εcaprolactone) (PCL) disc. (C) PCL disc. (d) PCL + poly(ethylene glycol) diacrylate disc

and with lower effect size for PGS+PCL [F (6, 12) = 5.82, p = 0.005, η_p^2 = 0.744, (1 − β) = 0.952] and PEGDA+PCL [F (6, 12) = 3.32, p = 0.036, η_p^2 = 0.624, (1 − β) = 0.749]. No significant effects were found for discopexy group [F (6, 12) = 2.65, p = 0.071, η_p^2 = 0.570, (1 − β) = 0.635]. Considering the differences in relation to the baseline (T0), the within-subject contrasts identified a statistically significant increase for PCL between T0 and T1, F (1, 2) = 60.99, p = 0.016, effect size of η_p^2 = 0.968, (1 − β) = 0.951. Lower increases were also found for PEGDA+PCL [F (1, 2) = 14.94, p = 0.061, η_p^2 = 0.882, (1 − β) = 0.541] and for PGS+PCL [F (1, 2) = 13.05, p = 0.069, η_p^2 = 0.867; (1 − β) = 0.497]. For PEGDA+PCL significant increases was also found for T2 and T3, F (1, 2) = 43.93 and 37.96, η_p^2 = 0.956 and 0.950, $p \leq$ 0.025, (1 − β) $\geq$ 0.851. No differences were found for discopexy ($p \geq$ 0.154) and for all groups when comparing baseline (T0) with T6 ($p \geq$ 0.078) Table S3.

3.4.2 | Rumination time per cycle

Cross-sectional analysis: rumination time per cycle rate did not vary across groups both in the pre-hoc test (T0) and in all times for the post-hoc test ($p > 0.05$), as shown in Table S4.

Longitudinal analysis: a one-way ANOVA with repeated measures was performed, taking as within-subject effects the baseline (T0) and the 6 months after surgery (T1 to T6) for PGS+PCL, PCL, PCL +PEGDA, and discopexy groups (Figure S11). Significant effects across time were found for PCL+PEGDA [F (6, 12) = 3.23, p = 0.040, η_p^2 = 0.617, (1 − β) = 0.983] and PCL [F (6, 12) = 7.19, p = 0.002, η_p^2 = 0.782, (1 − β) = 0.983], but not for PGS+PCL [F (6, 12) = 2.37, p = 0.096, η_p^2 = 0.542, (1 − β) = 0.581].

3.4.3 | Rumination kinematics area

Cross-sectional analysis: rumination areas varied across groups from T2 to T6 (Table S5).

Dunnett post-hoc test in T2 showed significant lower rumination area in PGS+PCL and PCL+PEGDA in comparison with discopexy group (Mean differences of −4002.3 and −7403.7, respectively, SE = 1096.0, $p \leq$ 0.016). Rumination area in PCL showed to be no different from the same area in discopexy and in PGS+PCL (p = 0.373). Rumination area in PCL was significantly higher in comparison with PCL+PEGDA (Mean difference = 5783.7, SE = 1096.0, p = 0.004). PGS+PCL and PCL+PEGDA didn't vary concerning rumination area (p = 0.088). In T3: PGS+PCL, PCL and PCL+PEGDA obtained significantly lower areas in comparison with discopexy group (Mean differences of −4550.0, −4295.0, and −6043.3, respectively, SE = 1181.4, $p \leq$ 0.017). Dunnett post-hoc test in T4 showed significant lower rumination area in PGS+PCL and PCL+PEGDA in comparison with discopexy group (Mean differences of −2945.0 and −4679.3, respectively, SE = 785.7, $p \leq$ 0.014). PCL and discopexy group showed no significant different rumination areas (p = 0.071). Rumination areas for PGS+PCL, PCL +PEGDA and PCL, were found to be similar across these groups ($p \geq$ 0.064).

A significant difference was found in T5, between PCL+PEGDA and discopexy (Mean difference = −5323.7, SE = 1252.9, p = 0.007), and between PCL and discopexy group (Mean difference = −3581.7, SE = 1252.9, p = 0.052). All the remaining comparisons didn't show significant differences in rumination areas across groups ($p \geq$ 0.127). In T6: PGS+PCL, PCL and PCL+PEGDA obtained significantly lower areas in comparison with discopexy group (Mean differences of

TABLE 2 The summary of ruminant kinetics measurements of sheep jaw movement extracted from videos while the sheep is ruminating

| Sheep ID | Date of birth | Baseline (mean of three measures) | | | | Allocation |
		Weight (kg)	Absolute masticatory time (s)[a]	Ruminant kinematics and area (pixels)[b]	Ruminant time per cycle (s)[c]	Randomized process
1545	August 12, 2014	52.6	99.3	5664	0.67	PGS+PCL disc
8553	November 10, 2011	66.3	86	7981	0.79	PGS+PCL disc
9981	September 2, 2012	66.3	88.3	6253	0.78	PGS+PCL disc
9983	September 5, 2012	52	66	5996	0.67	PCL+PEGDA disc
1615	November 6, 2011	63	83.3	8103	0.88	PCL+PEGDA disc
8258	July 11, 2012	72	62	7880	0.82	PCL+PEGDA disc
6984	August 9, 2014	46	116	6476	0.74	PCL disc
8254	July 23, 2010	54.6	86.3	7064	1.18	PCL disc
8574	November 11, 2011	57	81.3	5968	0.90	PCL disc

Abbreviations: PCL, poly(εcaprolactone); PCL+PEGDA, poly(εcaprolactone) + poly(ethylene glycol) diacrylate; PGS+PCL, poly(glycerol sebacate) + poly(εcaprolactone).

[a]The absolute masticatory time was measured from 9:00 a.m., when a dose of 150 g of dry pellets (*Rico Gado A3*) was introduced in the feeder, until all pellets were eaten.

[b]Ruminant kinematics refers to the average tracking of 15 ruminant cycles and the creation of a geometric form using the software *Image J*.

[c]A Canon 7D video camera set at 25 frames per second was used to record 15 ruminatory cycles, approximately 4 h after the 150 g feed. The number of frames per cycle was divided by 25 to obtain the time in seconds per cycle.

−4810.7, −5545.0, and −7585.3, respectively, SE = 1123.4, $p \leq 0.007$), however, no significant differences were found in rumination areas between PGS+PCL, PCL, and PCL+PEGDA ($p > 0.233$).

Longitudinal analysis: a one-way ANOVA with repeated measures was performed, taking as within-subject effects in baseline period (T0) and after surgery (T1 to T6) for PGS+PCL, PCL, PCL+PEGDA, and discopexy group (Figure S12). Significant effects across time were found for PGS+PCL [$F (6, 12) = 4.38$, $p = 0.014$, $\eta_p^2 = 0.687$, $(1 − \beta) = 0.870$], PCL [$F (6, 12) = 3.10$, $p = 0.045$, $\eta_p^2 = 0.608$, $(1 − \beta) > 0.714$], and PCL/PEGDA [$F (6, 12) = 3.70$, $p = 0.026$, $\eta_p^2 = 0.649$, $(1 − \beta) = 0.799$], but not for discopexy [$F (6, 12) = 1.35$, $p = 0.310$, $\eta_p^2 = 0.402$, $(1 − \beta) = 0.342$]. Considering the differences in relation to the baseline (T0), the within-subject contrasts identified a statistically significant difference for PCL+PEGDA between T0 and T2 to T6 [$F (1, 2)$ between 16.22 and 105.8, $p \leq 0.056$, effect sizes between $\eta_p^2 = 0.890$ and 0.981, $(1 − \beta)$ between 0.569 and 0.995]. Lower differences between T0 and T6 were also found for PGS+PCL [$F (1, 2) = 15.96$, $p = 0.057$, $\eta_p^2 = 0.889$, $(1 − \beta) = 0.564$] and for PCL [$F (1, 2) = 12.74$, $p = 0.070$, $\eta_p^2 = 0.864$; $(1 − \beta) = 0.490$]. No differences were found for discopexy group ($p \geq 0.289$).

3.5 | Multi-organ histologic results

Lungs were affected by granuloma parasites and nematodes compatible with *Cystocaulus ocreatus* or *Muellerius capillaris*. Some livers also revealed the presence of granuloma parasites compatible with fasciola hepatica migration. All the hearts presented Sarcocystis. No interposal biomaterials particles were observed in the studied organs (Figure S4).

4 | DISCUSSION

This work is original on the study design, using a randomized, blinded, preclinical study in TMJ domain, that follows ARRIVE guidelines and to our knowledge it is the first to include bilateral approach with an independent control group, minimizing possible bias. In TEMPOJIMS phase 2 the authors aimed to examine potential effects induced by three different interposal biomaterials using discopexy group as a control.

Discopexy is a common TMJ surgical technique, carefully used in this study as a control group to minimize the surgical bias and accurately measure the interposal biomaterial effect in the joint. From our previous study TEMPOJIMS phase 1, bilateral discopexy induced histological changes in cartilage and synovial without statistical significance when compared with the sham control group, showing a surgical intervention in the TMJ results in some level of intra-articular minor damage (Ângelo et al., 2018).

In this study, the authors did not find histological significant statistical difference in most of the outcomes studied between PGS+PCL and discopexy. A significant statistical difference between PGS+PCL and PCL+PEGDA was observed in cell shape, condylar surface

and superficial cartilage layer in mandible AC lamina. Major significant differences were observed in PCL versus discopexy. Temporal surface presented significant differences in AC lamina cell number, and in subchondral bone, the osteoblast activation and vascular invasion presented significant differences in PCL versus discopexy.

Poly(εcaprolactone) interposal biomaterial, at our best knowledge, has not been used to regenerate the TMJ disc but several authors have performed interesting work in mandibular condyle regeneration. In 2017 (Wang et al., 2017), a biphasic scaffold was used to successfully regenerate minipig TMJ condyle with PCL/Hydroxyapatite (bone phase) and polyglycolic acid (PGA)/polylactic acid (PLA), cartilage phase. Although this group used PGA/PLA for cartilage regeneration and PCL for bone regeneration, we tested PCL for disc regeneration due to biomechanical properties. Our results were not satisfactory, mostly due the breakdown of the PCL material (Figure 4d). The scaffold used by Wang (Wang et al., 2017), was seeded with chondrocytes and bone marrow stem cells. We used a different technique with a pure cell-free PCL, but this difference should not justify the material breakdown. One significant, and in our opinion, resemblance in both studies was the exact replica of the anatomic shape of the scaffold by 3D printing to mimic the native anatomy. The degradation of PCL is slow. A study in rats showed that PCL scaffold with an initial molecular weight of 66,000 remained intact in shape during the 2-year implantation. It degraded into low-molecular-weight (8000) pieces only at the end of 30 months (Poveda et al., 2007). This data is consistent with our results, the degradation of PCL was not completed in 6 months. By seeding it with bone morphogenetic protein-7 it has altered fibroblasts, and the tested group by Hollister group achieved compressive moduli and yield strengths for human trabecular bone (Murphy et al., 2013). Another study from the same group has reported that biphasic PCL scaffolds can be seeded with transformed fibroblasts and fully differentiated chondrocytes. This has provided tissues with a mineralized interface. Plus, the existence of blood vessels, marrow stroma, and adipose tissue have exposed a ceramic phase in these scaffolds. As a second strategy, the Mao group has shown the hidden potential of sequential photopolymerization of poly(ethylene glycol) hydrogels (Alhadlaq et al., 2004). Through this strategy, osteochondral constructs were obtained with condyle model shape. More importantly, this group has demonstrated the potential of inducing differentiation of primary bone-marrow-derived mesenchymal stem cells into chondrocyte to develop stratified bone and cartilage layers (Alhadlaq et al., 2004; Murphy et al., 2013). Finally, PCL seems a promising biomaterial for bone regeneration but not for fibrocartilage.

Our findings are consistent with a study that shows that PGS+PCL is a promising scaffold on promoting regeneration of TMJ fibrocartilage (Hagandora et al., 2013). On this study, PGS+PCL has demonstrated total reabsorption and histologic and imaging results show a number of cell increase with respect to normal cartilage, and mild remodeling on the subchondral bone, which could correlate with a suitable bone remodeling. In histology outcomes, we have not seen the production of a foreign body immune response and capsule development on the PGS+PCL interposal biomaterial,

as it has been documented in, that exogenous scaffolds induce such reactions (Vapniarsky et al., 2018). The imaging outcomes based on scores evaluation have shown that discopexy and PGS+PCL have no significative differences in condyle and temporal bone changes. The evaluation of the imaging outcomes is consistent with the effects induced on TMJ by the surgical intervention (Ângelo, Morouço, et al., 2018). In TEMPOJIMS phase 1, imaging outcomes have shown minor changes in bilateral discopexy with no statistical significance, and significant degenerative changes, induced by bilateral discectomy (Ângelo et al., 2017). On body mass outcomes, discopexy and PGS+PCL were the only groups able to recover from the postoperative period, and capable of reaching almost the baseline (T0) level. To the extent of our knowledge, body mass doesn't seem to be one of the most fundamental outcomes, due to animal survival instinct.

Other authors implanted an autologous cartilage tissue-engineered to heal the TMJ disc, and have assessed the efficacy, by presenting a histologic image where the degenerative defect has reduced, resulting in conservation of the articular surfaces (Vapniarsky et al., 2018). Another author shows the presence of fibro-cartilaginous tissue formation, from the implantation of scaffolds loaded with DPSCs (dental pulp stem cells), which acts as a good substitute of TMJ disc, since it seems to increase storage and elastic modulus with values similar to native TMJ disc (Bousnaki et al., 2018). These studies might reinforce the use of a TE implant instead of a synthetic polymer used in our study. However, such strategies lack of medical translational applicability.

From the kinematics outcomes, our previous research in TEMPOJIMS phase 1 (Ângelo, Gil, et al., 2018) has concluded that mastication and rumination in black Merino sheep are outcomes that should be considered for functional evaluation. Bilateral discopexy did not induce significant functional analysis changes in mastication and rumination. Yet, bilateral discectomy induced major changes in jaw kinematics, although along the study masticatory time and rumination time per cycle normalized.

Regarding the absolute masticatory time, in phase 1 study the authors observed that discectomy increased the masticatory time by 28% in T1. The discopexy increased the time by 11.4%, elucidating about the TMJ intervention effects, even maintaining the TMJ disc. In phase 2, no differences were observed between the PGS+PCL group and the control group. In fact, the PGS+PCL group finished the study eating 30.1% faster than the baseline. This percentage suggests that these animals had no pain at TMJ level. Both PCL and PCL+PEGDA achieved a slower food intake with significant increases in masticatory time. Those changes were more detrimental to the PCL group. Corroborating the phase 1 data, the animals were slowly able to recover to baseline masticatory time. It suggests an immense ability to adapt, highlighting again, the importance of function over form (Poveda et al., 2007).

Regarding the rumination time per cycle, we observed that 2 animals from PCL+PEGDA stopped ruminating through T1 and T2. Similarly, we have previously detected that 1 animal from discectomy group stopped the rumination process in T1 and T2 (Ângelo, Gil, et al., 2018). This absence of rumination during a certain period is intricate, and further studies should clarify these biomechanical constraints. Regarding PGS+PCL and PCL groups, the authors did not observe significant changes during the study, and the mechanical behavior was similar to the control group. After 3 months a remodeling and adaptive process occur in sheep TMJ and all interposal biomaterials presented similar performance. By the end of the study, no significant differences were found in rumination time, showing that the animals were able to particulate food appropriately after the adaptation process.

Considering the rumination area, all experimental groups finished the study with smaller rumination area when compared with the control group. A relation exists between rumination time and area. Thus, possible bias should be considered, regarding if an animal is ruminating with lower time, it may be because the area is lower and not because he is faster. In T2 the authors observed significant smaller rumination area in PGS+PCL and PCL+PEGDA and in T3–T6 all the interposal biomaterials presented lower areas in comparison to the control group. PGS+PCL and PCL presented more appropriate behavior when compared to PCL+PEGDA across time. Considering that PCL would provide an adequate mechanical strength but high tension between the surfaces, the authors expected PEGDA to lubricate and diminish the tension and presenting better results. No differences were observed, demonstrating further development and optimization on these concepts combining mechanical and biological virtues.

Regarding kinematics outcomes, the absolute masticatory time on PGS+PCL and discopexy groups were able to recover from the postoperative period and reach the T0 level. On the rumination time per cycle, PCL, PCL+PEGDA, PGS+PCL and discopexy groups were all able to recover to its initial state in T0. However, in rumination kinematics area, discopexy group was the only to show increase during the postoperative period.

The present research has a major limitation, the small sample size and the non-evaluation of stress factors and biomarkers expression through inflammatory reactions, in order to analyze pain. Moreover, bioactive signals may also be used to encourage cell proliferation and biosynthesis, since it has been found that bFGF has a stimulatory effect on the proliferation of mandibular condylar chondrocytes over IGF-I and TGF-β1 treatments in monolayer culture (Murphy et al., 2013). Nonetheless, this would require further immunology and toxicology assessments in the follow-up method, during postoperative period (T1–T6). In fact, having a sample of three animals per implant is limited and may be insufficient to detect significant statistical outcomes, but both joints were operated and a total of six interposal biomaterials were tested in each group. Either way, due to the distinct features of the three types of biomaterials, the obtained data on histology, imaging, body mass, kinematics and multi-organ histologic analysis provides interesting insights for further research. In future studies, from kinematics outcomes, the absolute masticatory time seems to be the most crucial parameter to consider. Still, histology results were quite relevant to assess the performance of the interposal biomaterial and its effects on cartilage.

The imaging plays a key role to determine degenerative changes and OA on temporal and jaw bones.

This work recognizes the potential of PGS+PCL scaffold as a TMJ disc replacement and suggests that when selecting a biopolymer to interpose in TMJ, there should be an optimization in pore size, and a correct preclinical trial design. As evidence, at our knowledge there is an overabundance of possible synthetic interposal biomaterials for articular disc and condylar TE, but there are few preclinical data proposing the use in patient-specific morphology and function. Therefore, the optimization of biomechanical stimulation for the scaffold under culture, may have a great impact to mimic the physiological loading conditions, influencing the extracellular matrix architecture and deposition once implanted. These might be the key factors to develop a biomimetic interposal biomaterial, able to heal TMJ and to respond to medical needs.

5 | CONCLUSIONS

In this randomized controlled preclinical trial of TMJ disc interposal implants, no infections occurred after the operations, and none of the implants could regenerate a new autologous disc. However, PGS +PCL disc demonstrated to be a promising choice to interpose in TMJ because it seems to provide the cushioning function of the native disc while keeping some cortical bone layer, observed by histologic analysis. Its elastomeric properties may represent a significant feature to approximate the TMJ native disc properties. Apart from the TMJ damage induced by the surgical intervention, animals receiving PGS+PCL implants exhibited only small functional changes. With PGS+PCL implants, we observed preserved non-hyaline cartilage except in one case, where we found fusion of the disc into the condyle. All PGS+PCL interposal biomaterial was reabsorbed in 6 months.

The PCL+PEGDA and PCL implants showed significant detrimental functional changes when compared to the discopexy. These results reinforce that it is more effective to not interpose any material in the joint than to use an inappropriate material. Adding PEGDA altered biomechanical properties of PCL, improved the PCL characteristics. These effects should be explored in the future. PCL +PEGDA induced major OA, with significant changes in condylar and temporal articular surfaces. The PCL disc induced major OA in mandibular condyle with major changes in non-hyaline cartilage surface. With PCL we observed foreign body reaction in 40% of the joints. In both PCL and PCL+PEGDA, the interposal biomaterials were not reabsorbed in 6 months. An hybrid biomaterial solution will possibly be part of the future generation of interposal scaffolds, guiding to cell development as its support the joint loading.

CONFLICT OF INTERESTS

The authors declare that there is no conflict of interest. The research described in the manuscript is original, not presently under consideration for publication elsewhere, and free of conflict of interest.

AUTHOR CONTRIBUTIONS

All the listed authors were involved in drafting and revising the article critically and approved the final version to be published. David Faustino Ângelo, Joaquim Ferreira, Florencio Monje, Francisco Salvado, and Raúl González-Garcia designed the study and performed the surgical protocol. David Faustino Ângelo, Pedro Morouço, Carla Moura, and Nuno Alves contributed to data acquisition. Carla Moura, Jin Gao, and Yadong Wang were involved in the fabrication of the interposal biomaterials. Pedro Faísca, Monica López Peña, Maria Permuy, and Fernando Munñoz coordinated the histologic blinded scoring. Lia Neto and Rita Sousa contributed to imaging blinded scoring. Monica López Peña, Rúben Araújo and Henrique Cardoso contributed to data analysis. Fábio Santos and Sandra Cavaco contributed to the animal veterinary support during the investigation. David Faustino Ângelo, Pedro Morouço, and Yadong Wang contributed to manuscript preparation.

DATA AVAILABILITY STATEMENT

The data that supports the findings of this study are available in the supporting information of this article.

ORCID

David Faustino Ângelo 🔟 https://orcid.org/0000-0001-8411-9946

REFERENCES

Abramowicz, S., & Dolwick, M. F. (2010). 20-Year follow-up study of disc repositioning surgery for temporomandibular joint internal derangement. *Journal of Oral and Maxillofacial Surgery*, 68(2), 239–242. https://doi.org/10.1016/j.joms.2009.09.051

Ahtiainen, K., Mauno, J., Ellä, V., Hagström, J., Lindqvist, C., Miettinen, S., Ylikomi, T., Kellomäki, M., & Seppänen, R. (2013). Autologous adipose stem cells and polylactide discs in the replacement of the rabbit temporomandibular joint disc. *Journal of the Royal Society Interface/ the Royal Society*, 10(85), 20130287. https://doi.org/10.1098/rsif.2013.0287

Alhadlaq, A., Elisseeff, J. H., Hong, L., Williams, C. G., Caplan, A. I., Sharma, B., Kopher, R. A., Tomkoria, S., Lennon, D. P., Lopez, A., & Mao, J. J. (2004). Adult stem cell driven genesis of human-shaped articular condyle. *Annals of Biomedical Engineering*, 32(7), 911–923. https://doi.org/10.1023/b:abme.0000032454.53116.ee

Alonso, A., Kaimal, S., Look, J., Swift, J., Fricton, J., Myers, S., & Kehl, L. (2009). A quantitative evaluation of inflammatory cells in human temporomandibular joint tissues from patients with and without implants. *Journal of Oral and Maxillofacial Surgery*, 67(4), 788–796. https://doi.org/10.1016/j.joms.2008.09.010

Ângelo, D. F., Gil, F. M., González-García, R., Mónico, L., Sousa, R., Neto, L., Caldeira, I., Moura, C., Francisco, L. C., Sanz, D., Alves, N., Salvado, F., & Morouço, P. (2018). Effects of bilateral discectomy and bilateral discopexy on black Merino sheep rumination kinematics: TEMPOJIMS—Phase 1—Pilot blinded, randomized preclinical study. *Journal of Cranio-Maxillofacial Surgery*, 46(2), 346–355. https://doi.org/10.1016/j.jcms.2017.11.022

Ângelo, D. F., Monje, F. G., González-García, R., Little, C. B., Mónico, L., Pinho, M., Santos, F. A., Carrapiço, B., Gonçalves, S. C., Morouço, P., Alves, N., Moura, C., Wang, Y., Jeffries, E., Gao, J., Sousa, R., Neto, L. L., Caldeira, D., & Salvado, F. (2017). Bioengineered temporomandibular joint disk implants: Study protocol for a two-phase exploratory randomized preclinical pilot trial in 18 black Merino sheep (TEMPOJIMS). *JMIR Research Protocols*, 6(3), e37. https://doi.org/10.2196/resprot.6779

Angelo, D. F., Morouço, P., Alves, N., Viana, T., Santos, F., González, R., Monje, F., Macias, D., Carrapiço, B., Sousa, R., Cavaco-Gonçalves, S., Salvado, F., Peleteiro, C., & Pinho, M. (2016). Choosing sheep (Ovis aries) as animal model for temporomandibular joint research: Morphological, histological and biomechanical characterization of the joint disc. *Morphologie*, 100(331), 223–233. https://doi.org/10.1016/j.morpho.2016.06.002

Ângelo, D. F., Morouço, P., Gil, F. M., Mónico, L., González-Gárcia, R., Sousa, R., Neto, L., Caldeira, I., Smith, M., Smith, S., Sanz, D., Abade dos Santos, F., Pinho, M., Carrapiço, B., Cavaco, S., Moura, C., Alves, N., Salvado, F., & Little, C. (2018). Preclinical randomized controlled trial of bilateral discectomy versus bilateral discopexy in Black Merino sheep temporomandibular joint: TEMPOJIMS—Phase 1—Histologic, imaging and body weight results. *Journal of Cranio-Maxillofacial Surgery*, 46(4), 688–696. https://doi.org/10.1016/j.jcms.2018.01.006

Annabi, N., Fathi, A., Mithieux, S. M., Weiss, A. S., & Dehghani, F. (2011). Fabrication of porous PCL/elastin composite scaffolds for tissue engineering applications. *The Journal of Supercritical Fluids*, 59, 157–167. https://doi.org/10.1016/j.supflu.2011.06.010

Bjørnland, T., & Larheim, T. A. (2003). Discectomy of the temporomandibular joint: 3-year follow-up as a predictor of the 10-year outcome. *Journal of Oral and Maxillofacial Surgery*, 61(1), 55–60. https://doi.org/10.1053/joms.2003.50010

Bousnaki, M., Bakopoulou, A., Papadogianni, D., Barkoula, N.-M., Alpantaki, K., Kritis, A., Chatzinikolaidou, M., & Koidis, P. (2018). Fibro/chondrogenic differentiation of dental stem cells into chitosan/alginate scaffolds towards temporomandibular joint disc regeneration. *Journal of Materials Science: Materials in Medicine*, 29(7), 97. https://doi.org/10.1007/s10856-018-6109-6

Brown, B. N., Chung, W. L., Almarza, A. J., Pavlick, M. D., Reppas, S. N., Ochs, M. W., Russell, A. J., & Badylak, S. F. (2012). Inductive, scaffold-based, regenerative medicine approach to reconstruction of the temporomandibular joint disk. *Journal of Oral and Maxillofacial Surgery*, 70(11), 2656–2668. https://doi.org/10.1016/j.joms.2011.12.030

Browning, M. B., Cereceres, S. N., Luong, P. T., & Cosgriff-Hernandez, E. M. (2014). Determination of the *in vivo* degradation mechanism of PEGDA hydrogels. *Journal of Biomedical Materials Research: Part A*, 102(12), 4244–4251. https://doi.org/10.1002/jbm.a.35096

Candirli, C., Demirkol, M., Yilmaz, O., & Memis, S. (2017). Retrospective evaluation of three different joint surgeries for internal derangements of the temporomandibular joint. *Journal of Cranio-Maxillofacial Surgery*, 45(5), 775–780. https://doi.org/10.1016/j.jcms.2017.02.003

Chin, A. R., Gao, J., Wang, Y., Taboas, J. M., & Almarza, A. J. (2018). Regenerative potential of various soft polymeric scaffolds in the temporomandibular joint condyle. *Journal of Oral and Maxillofacial Surgery*, 76(9), 2019–2026. https://doi.org/10.1016/j.joms.2018.02.012

Choi, J. R., Yong, K. W., Choi, J. Y., & Cowie, A. C. (2019). Recent advances in photo-crosslinkable hydrogels for biomedical applications. *BioTechniques*, 66(1), 40–53. https://doi.org/10.2144/btn-2018-0083

Cohen, J. (1988). *Statistical power analysis for the behavioral sciences.* Routledge Academic. https://doi.org/10.4324/9780203771587

Dolwick, M. F. (2001). Disc preservation surgery for the treatment of internal derangements of the temporomandibular joint. *Journal of Oral and Maxillofacial Surgery*, 59(9), 1047–1050. https://doi.org/10.1053/joms.2001.26681

Dong, L., Wang, S.-J., Zhao, X.-R., Zhu, Y.-F., & Yu, J.-K. (2017). 3D-printed poly(ε-caprolactone) scaffold integrated with cell-laden chitosan hydrogels for bone tissue engineering. *Scientific Reports*, 7(1), 13412. https://doi.org/10.1038/s41598-017-13838-7

Eriksson, L., & Westesson, P. L. (1987). Results of temporomandibular joint diskectomies in Sweden 1965-85. *Swedish Dental Journal*, 11(1–2), 1–9.

Eriksson, L., & Westesson, P.-L. (2001). Discectomy as an effective treatment for painful temporomandibular joint internal derangement: A 5-year clinical and radiographic follow-up. *Journal of Oral and Maxillofacial Surgery*, 59(7), 750–758. https://doi.org/10.1053/joms.2001.24288

Garrigues, N. W., Little, D., Sanchez-Adams, J., Ruch, D. S., & Guilak, F. (2014). Electrospun cartilage-derived matrix scaffolds for cartilage tissue engineering. *Journal of Biomedical Materials Research: Part A*, 102(11), 3998–4008. https://doi.org/10.1002/jbm.a.35068

Hagandora, C. K., & Almarza, A. J. (2012). TMJ disc removal. *Journal of Dental Research*, 91(8), 745–752. https://doi.org/10.1177/0022034512453324

Hagandora, C. K., Gao, J., Wang, Y., & Almarza, A. J. (2013). Poly (glycerol sebacate): A novel scaffold material for temporomandibular joint disc engineering. *Tissue Engineering: Part A*, 19(5–6), 729–737. https://doi.org/10.1089/ten.tea.2012.0304

Hall, M. B. (1984). Meniscoplasty of the displaced temporomandibular joint meniscus without violating the inferior joint space. *Journal of Oral and Maxillofacial Surgery*, 42(12), 788–792. https://doi.org/10.1016/0278-2391(84)90346-X

Hartman, L. C., Bessette, R. W., Baier, R. E., Meyer, A. E., & Wirth, J. (1988). Silicone rubber temporomandibular joint (TMJ) meniscal replacements: Postimplant histopathologic and material evaluation. *Journal of Biomedical Materials Research*, 22(6), 475–484. https://doi.org/10.1002/jbm.820220604

Holmlund, A. B. (1993). Surgery for TMJ internal derangement. *International Journal of Oral and Maxillofacial Surgery*, 22(2), 75–77. https://doi.org/10.1016/S0901-5027(05)80806-9

Lai, W. F., Stockstill, J. W., Deng, W.-P., Bowley, J., & Burch, J. G. (2001). Evaluation of biomechanical properties of Expanded-Polytetrafluoroethylene Soft Tissue Patch after dorsal implantation in the rat to mimic TMJ lateral reconstruction. *Journal of Oral Rehabilitation*, 28(3), 257–266. http://www.ncbi.nlm.nih.gov/pubmed/11394372

Li, H., Sun, S., Fan, B., Shen, P., Zheng, J., & Zhang, S. (2017). Prevention of adhesions in the temporomandibular joint by the use of chitosan membrane in goats. *British Journal of Oral and Maxillofacial Surgery*, 55(1), 26–30. https://doi.org/10.1016/j.bjoms.2016.08.017

Liu, X., Zheng, J., Cai, X., Abdelrehem, A., & Yang, C.(2018). Techniques of Yang's arthroscopic discopexy for temporomandibular joint rotational anterior disc displacement. *International Journal of Oral and Maxillofacial Surgery*, 48(6), 769-778. https://doi.org/10.1016/j.ijom.2018.12.003

McCarty, W. L., & Farrar, W. B. (1979). Surgery for internal derangements of the temporomandibular joint. *The Journal of Prosthetic Dentistry*, 42(2), 191–196. https://doi.org/10.1016/0022-3913(79)90174-4

Mercuri, L. G., Campbell, R. L., & Shamaskin, R. G. (1982). Intra-articular meniscus dysfunction surgery. *Oral Surgery, Oral Medicine, Oral Pathology*, 54(6), 613–621. https://doi.org/10.1016/0030-4220(82)90073-1

Miloro, M., McKnight, M., Han, M. D., & Markiewicz, M. R. (2017). Discectomy without replacement improves function in patients with internal derangement of the temporomandibular joint. *Journal of*

Cranio-Maxillofacial Surgery, *45*(9), 1425–1431. https://doi.org/10.1016/j.jcms.2017.07.003

Morouço, P., Biscaia, S., Viana, T., Franco, M., Malça, C., Mateus, A., Moura, C., Ferreira, F. C., Mitchell, G., & Alves, N. M. (2016). Fabrication of poly(ε-caprolactone) scaffolds reinforced with cellulose nanofibers, with and without the addition of hydroxyapatite nanoparticles. *BioMed Research International*, *2016*, 1–10. https://doi.org/10.1155/2016/1596157

Murphy, M. K., MacBarb, R. F., Wong, M. E., & Athanasiou, K. A. (2013). Temporomandibular disorders: A review of etiology, clinical management, and tissue engineering strategies. *The International Journal of Oral & Maxillofacial Implants*, *28*(6), e393–e414. Available at: http://www.ncbi.nlm.nih.gov/pubmed/24278954

Musumeci, G., Loreto, C., Carnazza, M. L., Strehin, I., & Elisseeff, J. (2011). OA cartilage derived chondrocytes encapsulated in poly(ethylene glycol) diacrylate (PEGDA) for the evaluation of cartilage restoration and apoptosis in an in vitro model. *Histology & Histopathology*, *26*(10), 1265–1278. https://doi.org/10.14670/HH-26.1265

Musumeci, G., Loreto, C., Castorina, S., Imbesi, R., Leonardi, R., & Castrogiovanni, P. (2013). New perspectives in the treatment of cartilage damage. Poly(ethylene glycol) diacrylate (PEGDA) scaffold. A review. *Italian Journal of Anatomy and Embryology/Archivio italiano di anatomia ed embriologia*, *118*(2), 204–210. http://www.ncbi.nlm.nih.gov/pubmed/25338410

Poveda, R. R., Bagan, J. V., Díaz Fernández, J. M., Hernández Bazán, S., & Jiménez Soriano, Y. (2007). Review of temporomandibular joint pathology. Part I: Classification, epidemiology and risk factors. *Medicina Oral, Patologia Oral y Cirugia Bucal*, *12*(4), E292–E298.

Renapurkar, S. K. (2018). Discectomy versus disc preservation for internal derangement of the temporomandibular joint. *Oral and Maxillofacial Surgery Clinics of North America*, *30*(3), 329–333. https://doi.org/10.1016/j.coms.2018.05.002

Schliephake, H., Schmelzeisen, R., Maschek, H., & Haese, M. (1999). Long-term results of the use of silicone sheets after diskectomy in the temporomandibular joint: Clinical, radiographic and histopathologic findings. *International Journal of Oral and Maxillofacial Surgery*, *28*(5), 323–329. https://doi.org/10.1016/S0901-5027(99)80074-5

Soni, A. (2019). Arthrocentesis of temporomandibular joint—Bridging the gap between non-surgical and surgical treatment. *Annals of Maxillofacial Surgery*, *9*(1), 158–167. https://doi.org/10.4103/ams.ams_160_17

Spagnoli, D., & Kent, J. N. (1992). Multicenter evaluation of temporomandibular joint Proplast-Teflon disk implant. *Oral Surgery, Oral Medicine, Oral Pathology*, *74*(4), 411–421. https://doi.org/10.1016/0030-4220(92)90285-X

Springer, I. N. G., Fleiner, B., Jepsen, S., & Açil, Y. (2001). Culture of cells gained from temporomandibular joint cartilage on non-absorbable scaffolds. *Biomaterials*, *22*(18), 2569–2577. https://doi.org/10.1016/S0142-9612(01)00148-X

Tucker, M. R., & Burkes, E. J. (1989). Temporary silastic implantation following discectomy in the primate temporomandibular joint. *Journal of Oral and Maxillofacial Surgery*, *47*(12), 1290–1295. https://doi.org/10.1016/0278-2391(89)90726-X

Urban, R. M., Jacobs, J. J., Tomlinson, M. J., Gavrilovic, J., Black, J., & Peoc'h, M. (2000). Dissemination of wear particles to the liver, spleen, and abdominal lymph nodes of patients with hip or knee replacement*. *The Journal of Bone & Joint Surgery—American Volume*, *82*(4), 457–477. https://doi.org/10.2106/00004623-200004000-00002

Vapniarsky, N., Huwe, L. W., Arzi, B., Houghton, M. K., Wong, M. E., Wilson, J. W., Hatcher, D. C., Hu, J. C., & Athanasiou, K. A. (2018). Tissue engineering toward temporomandibular joint disc regeneration. *Science Translational Medicine*, *10*(446), eaaq1802. https://doi.org/10.1126/scitranslmed.aaq1802

Walker, R. V., & Kalamchi, S. (1987). A surgical technique for management of internal derangement of the temporomandibular joint. *Journal of Oral and Maxillofacial Surgery*, *45*(4), 299–305. https://doi.org/10.1016/0278-2391(87)90347-8

Wang, F., Hu, Y., He, D., Zhou, G., Yang, X., & Ellis, E. (2017). Regeneration of subcutaneous tissue-engineered mandibular condyle in nude mice. *Journal of Cranio-Maxillo-Facial Surgery : Official Publication of the European Association for Cranio-Maxillo-Facial Surgery*, *45*(6), 855–861. https://doi.org/10.1016/j.jcms.2017.03.017

Wang, L., Lazebnik, M., & Detamore, M. S. (2009). Hyaline cartilage cells outperform mandibular condylar cartilage cells in a TMJ fibro-cartilage tissue engineering application. *Osteoarthritis and Cartilage*, *17*(3), 346–353. https://doi.org/10.1016/j.joca.2008.07.004

Widmark, G., Dahlström, L., Kahnberg, K.-E., & Lindvall, A.-M. (1997). Diskectomy in temporomandibular joints with internal derangement. *Oral Surgery, Oral Medicine, Oral Pathology, Oral Radiology, and Endodontology*, *83*(3), 314–320. https://doi.org/10.1016/S1079-2104(97)90235-3

Widmark, G., Gröndahl, H. G., Kahnberg, K.-E., & Haraldson, T. (1996). Radiographic morphology in the temporomandibular joint after diskectomy. *Cranio: The Journal of Craniomandibular & Sleep Practice*, *14*(1), 37–41. https://doi.org/10.1080/08869634.1996.11745947

SUPPORTING INFORMATION

Additional supporting information may be found online in the Supporting Information section at the end of this article.